AD-A193 765 A THEORETICAL INVESTIGATION OF LASER-SUSTAINED PLASMA THRUSTER(U) TENNESSEE UNIV SPACE INST TULLAHOMA CENTER FOR LASER APPLICAT.. S JENG ET AL. 21 APR 88 1/1

UNCLASSIFIED AFOSR-TR-88-0537 AFOSR-86-0317 F/G 21/3 NL

END

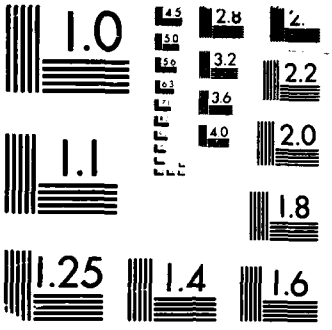

MICROCOPY RESOLUTION TEST CHART

AD-A193 765 OPY

(2)

DOCUMENTATION PAGE

Form Approved OMB No. 0704-0188

DTIC ELECTED MAY 20 1988 S D

1a. REPORT SECURITY CLASSIFICATION: Unclassified	1b. RESTRICTIVE MARKINGS
2a. SECURITY CLASSIFICATION AUTHORITY	3. DISTRIBUTION/AVAILABILITY OF REPORT: Approved for public release; distribution is unlimited
2b. DECLASSIFICATION/DOWNGRADING SCHEDULE	
4. PERFORMING ORGANIZATION REPORT NUMBER(S)	5. MONITORING ORGANIZATION REPORT NUMBER(S): AFOSR-TR- 88-0537
6a. NAME OF PERFORMING ORGANIZATION: Center for Laser Applications, Univ. of Tenn. Space Institute	6b. OFFICE SYMBOL (If applicable)
6c. ADDRESS (City, State, and ZIP Code): Tullahoma, TN 37388	7a. NAME OF MONITORING ORGANIZATION: AFOSR/NA
	7b. ADDRESS (City, State, and ZIP Code): Building 410, Bolling AFB DC 20332-6448
8a. NAME OF FUNDING/SPONSORING ORGANIZATION: AFOSR/NA	8b. OFFICE SYMBOL (If applicable): NA
	9. PROCUREMENT INSTRUMENT IDENTIFICATION NUMBER: AFOSR-86-0317
8c. ADDRESS (City, State, and ZIP Code): Building 410, Bolling AFB DC 20332-6448	10. SOURCE OF FUNDING NUMBERS: PROGRAM ELEMENT NO. 61102F; PROJECT NO. 2308; TASK NO A1; WORK UNIT ACCESSION NO.

11. TITLE (Include Security Classification)
(U) (AIAA-87-0383) "A Theoretical Investigation of Laser-Sustained Plasma Thruster"

12. PERSONAL AUTHOR(S)
Sam-You Jeng and Dennis Keefer

13a. TYPE OF REPORT	13b. TIME COVERED	14. DATE OF REPORT (Year, Month, Day)	15. PAGE COUNT
Pub.	FROM 9/1/86 TO 3/31/87	1988 April 21	11

16. SUPPLEMENTARY NOTATION

17. COSATI CODES			18. SUBJECT TERMS (Continue on reverse if necessary and identify by block number)
FIELD	GROUP	SUB-GROUP	thruster; laser-sustained; hydrogen; geometric; ray tracing; LTE; axisymmetric; Navier-Stokes

19. ABSTRACT (Continue on reverse if necessary and identify by block number)

A numerical code has been successfully developed for the investigation of thruster performance using a laser-sustained hydrogen plasma as the propellant. The plasma was sustained using a 10.6 μm CO_2 laser beam which is focused at different positions within the thruster. The physical model assumed that plasma is in thermodynamically equilibrium (LTE), and geometric ray tracing was adopted to describe the laser beam. The stead-state, axisymmetric, Navier-Stokes equations coupled with the laser power absorption process have been solved numerically. A pressure based Navier-Stokes numerical solver using body-fitted coordinates was used to calculate the laser-supported rocket flow which includes both subsonic and supersonic flow regions. From the limited parametric study, which did not try to optimize the rocket performance, it was found that better performance was obtained when the laser beam was focused closer to the rocket throat.

20. DISTRIBUTION/AVAILABILITY OF ABSTRACT	21. ABSTRACT SECURITY CLASSIFICATION
☒ UNCLASSIFIED/UNLIMITED ☒ SAME AS RPT ☒ DTIC USERS	Unclassified
22a. NAME OF RESPONSIBLE INDIVIDUAL: Dr Mitat Birkan	22b. TELEPHONE (Include Area Code): (202) 767-4936 / 22c. OFFICE SYMBOL: AFOSR/NA

DD Form 1473, JUN 86 Previous editions are obsolete. SECURITY CLASSIFICATION OF THIS PAGE

AIAA'87

AIAA-87-0383
A Theoretical Investigation of Laser-Sustained Plasma Thruster

San - Mou Jeng and Dennis Keefer
The University of Tennessee Space Institute
Tullahoma, TN

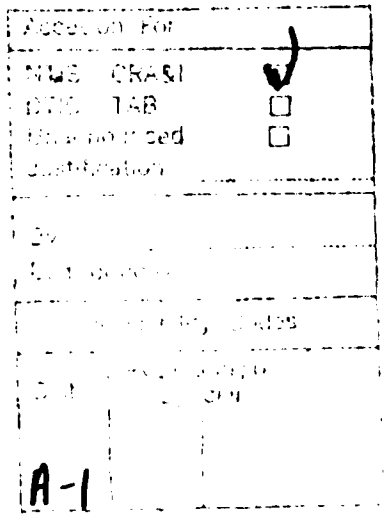

AIAA 25th Aerospace Sciences Meeting
January 12-15, 1987/Reno, Nevada

A Theoretical Investigation of Laser-Sustained Plasma Thruster

San-Mou Jeng* and Dennis Keefer**

Center for Laser Applications
University of Tennessee Space Institute
Tullahoma, Tennessee 37388
(615) 455-0631 ext. 338

ABSTRACT

A numerical code has been successfully developed for the investigation of thruster performance using a laser-sustained hydrogen plasma as the propellant. The plasma was sustained using a 10.6μm CO_2 laser beam which is focused at different positions within the thruster. The physical model assumed that plasma is in thermodynamically equilibrium (LTE), and geometric ray tracing was adopted to describe the laser beam. The steady-state, axisymmetric, Navier-Stokes equations coupled with the laser power absorption process have been solved numerically. A pressure based Navier-Stokes numerical solver using body-fitted coordinates was used to calculate the laser-supported rocket flow which includes both subsonic and supersonic flow regions. From the limited parametric study, which did not try to optimize the rocket performance, it was found that better performance was obtained when the laser beam was focused closer to the rocket throat.

NOMENCLATURE

A	coefficient in difference equation for variable ϕ
I	laser ray intensity
J	Jacobian of inverse coordinate transformation
k	conductivity
p	pressure
q_1, q_2, q_3	geometric relations between coordinate systems
$\dot{q}$	emission coefficient for optically thin radiation
R, S, T	source term in equations 6, 7, 15, respectively
s	distance along laser ray
U, V	velocity component along $\varsigma-$ and $\eta-$axis, respectively
u, v	velocity component along $x-$ and $r-$axis, respectively
ς, η	axes of curvilinear coordinate system
ϕ	general dependent variable
ρ	density
Γ	effective diffusion coefficient
μ	viscosity
α	absorption coefficient

Subscript

E, W, N, S	four adjacent nodes to P
e, w, n, s	four surfaces of the control volume centered at P
i	laser ray i
P	nodal point to be solved in difference equation
rad	radiation
ς, η	partial derivative with respect to ς, η
ϕ	for dependent variable ϕ

Superscript

$*$	values based on given pressure field
$'$	corrected values according to corrected pressure field

INTRODUCTION

This paper describes the numerical calculations for a rocket using a laser-sustained plasma as the propellant for a propulsion device. The plasma is used to absorb and convert the power from a remote laser beam into the propellant which is expanded through a nozzle to generate the required thrust for a space vehicle. This kind of propulsion system is called laser-thermal propulsion. Several different modes of operating a laser-supported rocket have been proposed; for example, pulsed laser-supported detonation wave;[1] cw laser-sustained plasma (LSP).[2-4] In this paper, the discussion is limited to the numerical calculations of a rocket flow using a cw laser-sustained pure hydrogen plasma as the propellant.

A schematic of a proposed laser-supported rocket

---

* Assistant professor, Aerospace and Mechanical Engineering, Member AIAA

** Professor, Engineering Science and Mechanics, Member AIAA

UTSI Publication NO. E02-0115-006-87

thruster is shown in Figure 1. Laser power is absorbed by and sustains a high temperature plasma core (about 15,000-20,000 K), which mixes with the cold buffer flow of propellant downstream, heating the flow to the maximum temperature that the chamber wall material can tolerate. Then, the flow is accelerated through a conventional nozzle to produce the required thrust. Since the laser power absorption by a plasma is through inverse bremsstrahlung, any type of propellant can be used, and for propulsion purposes, the lowest molecular weight propellant, hydrogen, is the best candidate. The major advantages of this device, compared to chemical propulsion, are that the lowest molecular weight propellant can be used, and that the maximum temperature of the working fluid is not limited to the flame temperature of a combustion process. The combination of high temperature and a low molecular weight propellant results in a very high expected specific impulse. An estimated specific impulse for laser-sustained plasma propulsion using hydrogen propellant is in the range of 1000-1500 sec.,[5] which is about three times that of the most advanced chemical propulsion system.

The modeling of the LSP for propulsion began with the one-dimensional work of Raizer.[6] Several other studies[7,8] followed this analysis but used more sophisticated analytical and computational methods. Unfortunately, one-dimensional models have an inherent weakness. The LSP tends to be highly dependent on laser beam geometry, radial convection and radial diffusion transport of momentum and energy in the flow. Keefer and coworkers[9,10] developed a simplified semi-two-dimensional model which considered the radial energy diffusion but assumed that the laser beam and the streamlines were parallel. Later, Glumb and Krier[11] extended that model by using a converging laser beam, as well as using more realistic gas properties. However, their model still did not consider the momentum equations but, instead, assumed that the radial velocity was zero.

Merkle and coworkers[12,13] used a contemporary numerical method to attack the full two-dimensional problem. They succeeded in the calculation of a low temperature LSP (peak temperature about 4,000 K) in a low-mach number hydrogen flow seeded with cesium. It is feasible to extend their approach to a pure hydrogen plasma, but the higher peak temperature (about 16,000 K) and much stronger nonlinear optical properties of the pure hydrogen plasma can result in numerical stability problems.

Recently, Jeng and Keefer[14,15] obtained the numerical solutions for a rigorous two-dimensional model with realistic gas properties for the LSP in pure argon and pure hydrogen flows. Their results for the argon flows agree well with experimental data[16,17] in the prediction of plasma position, size, shape and peak temperature. Jeng et al[15,18,19] have also studied the effect of laser power, flow rate, static pressure and optical geometry on the LSP flows. Their work also indicated that there are no fatal errors in the laser propulsion concept, and the critical parameters of plasma size, position, radiation heat loss and energy conversion efficiency, can be controlled using an appropriate optical arrangement and a suitable flow configuration.

The objectives of the current study are to develop a new numerical code based on extended plasma model developed by Jeng and Keefer[14,15] for the real nozzle flow which includes both low and high mach number flows, and to conduct a preliminary parametric study of laser rocket performance. There was no attempt, in this paper, to determine the actual rocket performance. In the following section, the theoretical method used in the study is described. This is followed by a discussion of model calculations and some initial parametric studies.

THEORETICAL MODEL

LASER BEAM. Geometric optics were used to describe the laser beam which was assumed to be divided into a finite number of individual rays. Each ray path through the optical system to the plasma flow was calculated using real-ray tracing. Diffraction of the laser beam due to the finite aperture of the lens, and effects due to the inhomogeneous refractive index within the plasma were neglected in the calculation. The local intensity of each individual ray i was described by Beer's law written in the the following form.

$$\frac{dI_i}{ds_i} = -\alpha I_i \qquad (1)$$

where s_i is the distance along the laser propagation direction for ray i, and α is absorption coefficient at laser wavelength and depends on local plasma temperature and pressure.

PLASMA FLOW. The model assumed that the flow is laminar, steady-state, axisymmetric and has variable physical properties. The pressure of the plasma is relatively high so local thermodynamic equilibrium (LTE) for the plasma can be assumed with little error. Therefore, the plasma can be described by a single temperature, and its physical properties are only a function of this temperature and pressure. The model also considered the thermal radiation emitted from the plasma which included the contributions from free to free, free to bound, and bound to bound transitions. These radiation properties are a strong function of wavelength, and the current model adopted the simplified approach, developed by Kemp

et al[20] and Caledonià et al.[21] to solve the hydrogen plasma radiation transport equations. Radiation transport was divided into two parts depending on wavelength: for wavelengths longer than 0.095 μm, the optical depth is long and an optically thin approximation, in which all radiation escapes from the plasma, was used; and in other wavelength regions, the optical depth is short and an optically thick approximation, which can be described as a diffusion process, was assumed. Following the above assumptions, the equations of conservation of mass, momentum and energy for the flow can be written as :

$$\frac{\partial(\rho u)}{\partial x}+\frac{1}{r}\frac{\partial(r\rho v)}{\partial r}=0, \tag{2}$$

$$\frac{\partial(\rho uu)}{\partial x}+\frac{1}{r}\frac{\partial(r\rho uv)}{\partial r}=-\frac{\partial p}{\partial x}+\frac{\partial}{\partial x}\left(\mu\frac{\partial u}{\partial x}\right)$$
$$+\frac{1}{r}\frac{\partial}{\partial r}\left(\mu r\frac{\partial u}{\partial r}\right)+\frac{\partial}{\partial x}\left(\mu\frac{\partial u}{\partial x}\right)+\frac{1}{r}\frac{\partial}{\partial r}\left(\mu r\frac{\partial v}{\partial x}\right)$$
$$-\frac{\partial}{\partial x}\left[\frac{2\mu}{3}\left(\frac{\partial u}{\partial x}+\frac{1}{r}\frac{\partial(rv)}{\partial r}\right)\right], \tag{3}$$

$$\frac{\partial(\rho uv)}{\partial x}+\frac{1}{r}\frac{\partial(r\rho vv)}{\partial r}=-\frac{\partial p}{\partial r}+\frac{\partial}{\partial x}\left(\mu\frac{\partial v}{\partial x}\right)$$
$$+\frac{1}{r}\frac{\partial}{\partial r}\left(\mu r\frac{\partial v}{\partial r}\right)+\frac{\partial}{\partial x}\left(\mu\frac{\partial u}{\partial r}\right)+\frac{1}{r}\frac{\partial}{\partial r}\left(\mu r\frac{\partial v}{\partial r}\right)-\frac{2\mu v}{r^2}$$
$$-\frac{1}{r}\frac{\partial}{\partial r}\left[\frac{2\mu r}{3}\left(\frac{\partial u}{\partial x}+\frac{1}{r}\frac{\partial(rv)}{\partial r}\right)\right]+\frac{2\mu}{3r}\left(\frac{\partial u}{\partial x}+\frac{1}{r}\frac{\partial(rv)}{\partial r}\right), \tag{4}$$

$$\frac{\partial(\rho uh)}{\partial x}+\frac{1}{r}\frac{\partial(r\rho vh)}{\partial r}=\frac{\partial}{\partial x}\left(\frac{k_{eff}}{c_p}\frac{\partial h}{\partial x}\right)$$
$$+\frac{1}{r}\frac{\partial}{\partial r}\left(\frac{rk_{eff}}{c_p}\frac{\partial h}{\partial r}\right)-\frac{\partial\left(\rho u(\frac{1}{2}u^2+\frac{1}{2}v^2)\right)}{\partial x}$$
$$-\frac{\partial\left(r\rho v(\frac{1}{2}u^2+\frac{1}{2}v^2)\right)}{r\partial r}+\frac{4}{3}\mu\left(\left(\frac{\partial u}{\partial x}\right)^2+\left(\frac{\partial v}{\partial r}\right)^2\right)$$
$$+\mu\left(\left(\frac{\partial v}{\partial x}\right)^2+\left(\frac{\partial u}{\partial r}\right)^2\right)+\frac{4}{3}\mu\frac{\partial u}{\partial x}\frac{\partial v}{\partial r}+2\mu\frac{\partial v}{\partial x}\frac{\partial u}{\partial r}$$
$$+\frac{1}{r}\left(\frac{4}{3}\mu\frac{v^2}{r}-\frac{4}{3}\mu v\left(\frac{\partial v}{\partial x}+\frac{\partial v}{\partial r}\right)\right)$$
$$+\sum\alpha I_i-\dot{q}_{rad}, \tag{5}$$

where k_{eff} is the sum of molecular thermal conductivity and radiation-induced thermal conductivity in the optically thick limit; $\dot{q}_{rad}$ is radiative heat loss in the optically thin limit; $\alpha\Sigma I_i$ represents the local power addition from the laser beam to the flow; and as mentioned before, the physical properties involved in equations (2-5) are a function of the local temperatures and pressures. Reference 15 has a detailed description of the thermophysical and optical properties sources used in this work.

In the calculations, adiabatic, nonslip and zero emissivity conditions were assigned at the thruster wall. Total pressure, total temperature and zero radial velocity were specified at the inlet, and upstream running Riemann invariants extrapolation plus the isentropic relations were used to calculate other properties. At the exit, the properties were linearly extrapolated from the interior flow domain.

METHOD OF COMPUTATION

COORDINATE TRANSFORMATION. The set of transport equations (3-5) can be written in the cylindrical system coordinates for the dependent variable, ϕ, in the following generalized form:

$$\frac{\partial}{\partial x}(r\rho u\phi)+\frac{\partial}{\partial r}(r\rho v\phi)=\frac{\partial}{\partial x}(\Gamma^{\phi}r\frac{\partial\phi}{\partial x})$$
$$+\frac{\partial}{\partial r}(\Gamma^{\phi}r\frac{\partial\phi}{\partial r})$$
$$+r\cdot R^{\phi}(x,r), \tag{6}$$

where $\Gamma^{\phi}{}_{eff}$ is the effective diffusion coefficient and $R^{\phi}(x,r)$ is the source term. The source term for the momentum equations (3,4) also includes the diffusion terms from the dilation effect. When new independent variables ς and η are introduced, Eq. (6) changes according to the general transformation ς and η. A schematic illustration of the relations between the physical domain and the transformed domain is shown in Figure 2. Equation (6) is rewritten in ς and η coordinates as follows:

$$\frac{1}{J}\frac{\partial}{\partial\xi}(r\rho U\phi)+\frac{1}{J}\frac{\partial}{\partial\eta}(r\rho V\phi)=$$
$$\frac{1}{J}\frac{\partial}{\partial\xi}\left[\frac{\Gamma^{\phi}r}{J}(q_1\phi_{\xi}-q_2\phi_{\eta})\right]+\frac{1}{J}\frac{\partial}{\partial\eta}\left[\frac{\Gamma^{\phi}r}{J}(-q_2\phi_{\xi}+q_3\phi_{\eta})\right]$$
$$+r\cdot S^{\phi}(\xi,\eta) \tag{7}$$

where

$$U=ur_{\eta}-vx_{\eta}, \tag{8}$$

$$V=vx_{\xi}-ur_{\xi}, \tag{9}$$

$$q_1 = x_\eta^2 + r_\eta^2, \tag{10}$$

$$q_2 = x_\xi x_\eta + r_\xi r_\eta, \tag{11}$$

$$q_3 = x_\xi^2 + y_\xi^2, \tag{12}$$

$$J = x_\xi r_\eta - x_\eta r_\xi, \tag{13}$$

and $S^\phi(\varsigma, \eta)$ is the source term in the ς and η coordinates.

NUMERICAL . GORITHM A nonstaggered grid system, as shown in Figure 2, is adopted in the calculations. For a typical grid node P are enclosed in its cell and surrounded by its neighbors N, S, E, and W. The integral of Eq. 7 over its control volume, by arbitrary taking $\Delta\varsigma = 1$ and $\Delta\eta = 1$, becomes

$$\begin{aligned}(r\rho U\phi)_e - (r\rho U\phi)_w + (r\rho V\phi)_n - (r\rho V\phi)_s \\ = \left[\frac{r\Gamma^\phi}{J}(q_1\phi_\xi - q_2\phi_\eta)\right]_e - \left[\frac{r\Gamma^\phi}{J}(q_1\phi_\xi - q_2\phi_\eta)\right]_w \\ + \left[\frac{r\Gamma^\phi}{J}(-q_2\phi_\xi + q_3\phi_\eta)\right]_n - \left[\frac{r\Gamma^\phi}{J}(-q_2\phi_\xi + q_3\phi_\eta)\right]_s \\ + r \cdot J \cdot S^\phi(\varsigma, \eta),\end{aligned} \tag{14}$$

Second-order center differencing is used to discretize the above equation, except for the convective terms when the cell Reynolds number is greater than 2. In that case, first order upwind differencing is used for the convective terms. A staggered grid system, for body-fitted coordinates, has been widely used,[22] and it has been known that an oscillatory field will be produced using the nonstaggered grid system. The artificial viscosity term proposed by Rhie and Chow[23] to cure the problem was also implemented in this study. The cross derivatives in the diffusion terms of Eq. (14) are the results of the nonorthogonal coordinate system and are usually small. In order to use the solution procedure for the five-point unknowns, these terms are combined with the source term and treated as known quantities and the resulting relation between ϕ_P and the neighboring values can be written as :

$$\begin{aligned}A_P\phi_P = A_E\phi_E + A_W\phi_W + A_N\phi_N + A_S\phi_S \\ + r \cdot J \cdot T^\phi(\varsigma, \eta),\end{aligned} \tag{15}$$

where the coefficients A involve the flow properties of convection, diffusion, area, etc., and $T^\phi(\varsigma, \eta)$ includes the source term $S^\phi(\varsigma, \eta)$ and the cross derivatives in the diffusion terms.

PRESSURE CORRECTION PROCEDURE. While the general transport equation, Eq. (15), was used to solved momentum and energy equations, the pressure field must be solved using the continuity equation. The procedure used in this work is an adoption of algorithm developed by Rhie,[24] and only a brief discussion is presented in this section. The pressure equation used in the adopted procedure is similar to that of SIMPLER[25] and PISO,[26,27] except that the density term is treated implicitly for the compressible flow. The basic idea is to use the following relations to correct the mass flux obtained from momentum equations

$$\rho u = \rho^* u^* + \rho' u^* + \rho^* u' \tag{16}$$

$$\rho v = \rho^* v^* + \rho' v^* + \rho^* v' \tag{17}$$

and the discretized pressure equation becomes a transport equation for compressible flow instead of Poisson equation. The ratio of diffusion term to convection term is dependent on Mach number, and as Mach number increases, the convection term becomes dominant. The split operator concept similar to PISO was also adopted in the current study to solve the pressure correction equation.

RESULTS AND DISUCSSION

Figure 3 shows the thruster dimensions used in the calculations. It includes a cylindrical section upstream of the convergent-divergent nozzle. The throat and cylindrical diameters are 6 and 40.74 mm respectively, and the exit to throat area ratio is 6. The coordinate origin used to present the calculated results is at the center of the throat. Although Figure 1 shows that the hydrogen flows into the chamber radially, in the calculations reported here the inlet flow direction was assumed axial. The total pressure and total temperature were specified at the inlet. In the traditional chemical rocket, the total pressure has a minor effect on the expected value of the specific impulse, but in the laser-supported rocket, the pressure has a substantial influence on the absorption and radiation processes that directly affect the available enthalpy of the propellant and the specific impulse of the thruster. Based on our previous parametric studies[15] for laser-sustained hydrogen plasmas in a constant area pipe flow, it was found that 3 atm total pressure was adequate for the thruster upstream condition, and this value was used in the calculations. The total temperature at the inlet was specified as 1500K in the calculations, based on the expected use of a regenerative cycle to recover the optically thin radiation from plasma.

The focusing lens used in the calculations has a nominal focal length 203 mm, and References 14 and 15 has detailed discussion of this lens geometry. The actual dimensions of this lens were adopted in the ray

tracing for the laser beam, so the spherical aberration of the lens was also included in the calculations. The laser was assumed to have 10.6 μm wavelength and a collimated, 40 mm diameter Gaussian beam incident on the lens. The only preliminary parametric study of the rocket performance reported in this paper was to focus the laser beam at different axial locations using the same lens arrangement. Table 1 lists the operating conditions, including one case without laser power addition.

In the calculations, nonuniformly spaced grids in the physical space were transformed into uniformly spaced grids in both radial and axial directions in the transformed space, as illustrated in Figure 4. From previous studies [14,15,18,19] of LSP within a constant diameter pipe, the position of the high temperature plasma zone was found to be highly dependent on the flow configurations and the optical arrangements, and it was not easy to prelocate the region in the physical plane where a dense grid distribution was needed to accommodate the high temperature gradients. Therefore, a preliminary calculation was first performed for each case to locate the high temperature zone, then the grid distribution was refined and used for the final calculation.

The newly developed computer code was first used to calculate the thruster flow without considering laser heat addition, and the results were used to check the behavior of the computer program and to serve as benchmark to compare with the other calculated cases which included the laser heat addition. The Mach number contours for case no. 1 are shown in Figure 5. Because the nozzle expansion angle is only 6°, the contours outside of the wall where diffusion transport is not important, are almost straight, and are similar to one-dimensional nozzle calculations. Since the nonslip condition was applied in the calculations, the Mach number near the wall is smaller than that near the centerline at the same axial location. This demonstrates that the newly developed computer program can also handle the boundary layer in supersonic flow. In this test case, there were only a few grids within the boundary, and we made no special attempt to resolve the boundary layer to good numerical accuracy. If needed, more grids can be included in that region and a more accurate solution can be obtained.

Figure 6 shows isotherms for case no. 2, and the outer laser beam boundary was also plotted in the figure as a dashed line. The plasma core is located upstream of the laser focus, and the distance between the laser focus and the high temperature plasma core, which depends on flow configurations and optical arrangements as discussed in the early section of this paper, is 10 mm. Downstream of the laser focus, the mixing process quickly reduces the centerline temperature. In the throat region, only a small portion of the hydrogen flow near the axis is heated, and a major portion of the flow is still unheated. For an optimized rocket, one of the design criteria is to have a uniformly distributed temperature at the throat in order to reduce the two-dimensional losses. In the calculated case, this condition was not satisfied. Near the wall of the nozzle exit, there is a local hot spot which is due to the viscous dissipation effect within the boundary layer.

Laser-sustained plasmas, operated at 30 kW laser power, absorb almost all of the incoming laser beam power. In the calculated case no. 2, only 397 W of laser power was transmitted through the plasma which either reached the thruster wall or was transmitted through the throat. The wall material could easily withstand this small level of transmitted power density. The optically thin radiation from the plasma is also an important factor for a laser-supported rocket design. It represents the portion of laser power that is not directly converted into the flow power. However, this radiation power, like a part of the transmitted laser power, will be absorbed by the wall, and by using a regenerative cycle, part of this energy can be recovered and used to heat the hydrogen from its storage temperature up to the propellant inlet temperature of the thruster. For case no. 2, the optically thin radiation was 17.9 kW which was only 30 % of the energy needed to heat hydrogen to the assigned inlet temperature, 1500 K.

Pressure and Mach number contours for case no. 2 are shown in Figure. 7 and Figure. 8, respectively. Pressure contours downstream of the laser focus in Figure 7 are similar to the calculated results for case no. 1. Those have only a very small radial variation and imply that the nonuniformly distributed temperature field has little effect on the pressure field. However, a high pressure zone, even higher than the inlet static pressure of the thruster ($3x10^5 N/m^2$), occurs ahead the high temperature plasma zone. The Mach number at the inlet is about 0.019 and the maximum calculated Mach number is 2.605 at the nozzle exit. The Mach number contours in the supersonic region are very complicated, compared to that of case. no. 1 in Figure 5, although the velocity monotonically increased from the wall to the centerline. The Mach number at the centerline is always smaller than away from the centerline, since the temperature, as well as sonic speed, is higher at the centerline. The unheated region still has very straight Mach number contours similar to those shown in Figure 5 for case no. 1. The mixing region between hot center flow and the colder unheated flow shows very complicated contours. Mixing in that region, which implies variations of sonic speed due to different temperature, molecular weight, and specific heat, are the major factors. The Mach

number near the wall is smallest due to the boundary effect, and the Mach number on the centerline is always smaller than that away from the centerline in the subsonic portion of the flow.

In the previous studies[15,16], it was found that laser heat addition to the flow will generate a very complicated velocity field, even in a constant area pipe. The same behavior was also observed in the current results. Figure 9 shows the radial velocity contours for case no. 2. Near the high temperature plasma core region, both positive and negative radial velocity occurs. In the supersonic region, a local minimum exists in the mixing zone between heated and unheated flow for case no. 2, and the radial velocity increases from the centerline up to the edge of the boundary for the unheated case no. 1. Nonuniformly distributed temperature at the throat is the main cause for the above results.

Figure 10(a) and 10(b) show isotherms for cases no.4 and no. 5, respectively. Their laser focuses are closer to the throat than case no. 2, and the focus is within the nozzle contracting section for case no. 5. As the laser focus moves closer to the throat, the size of the plasma becomes smaller. Since the optically thin radiation is proportional to the plasma size, the radiation loss for case no. 5, 9.9 kW, is much smaller than 15.9 kW and 18.6 kW for cases no.4 and no. 2, respectively. Because the transmitted laser power is small and similar for all cases, the energy directly converted to the flow is highest for case no. 5. The laser beam also heats a larger portion of the flow at the throat in case no. 5 than other cases, and this produces better thruster performance.

Table 2 lists the calculated properties for the five test cases. The optically thin radiation heat loss ranges from 61 % to 33 % of the laser power, and the transmitted laser power is relatively small by comparison. The peak axial velocity, which is always located on the centerline at the exit, increases from 4763 m/sec for the unheated thruster to 18957 m/sec for case no. 5. The maximum temperature of the plasma shows little dependence on the variation of laser focal position among the test cases. The peak Mach number at the exit plane is located within the unheated flow for all test cases, and it increases as the laser focal point moves downstream. The mass flow rate decreases as the laser focal point moves toward the throat.

SUMMARY AND CONCLUSIONS

The flow within a laser-sustained plasma rocket thruster has been successfully calculated. The physical model was based on steady-state two-dimensional Navier-Stokes equations for the flow and geometric real-ray tracing for the laser beam. Realistic thermophysic and optical properties based on locally thermodynamical equilibrium assumptions were incorporated into the calculations, and radiation heat transfer from the plasma was simplified using optically thin and optically thick assumptions. The governing equations were first transformed into body-fitted coordinates and were solved numerically. A pressure-based Navier-Stokes solver with a split operator concept was used for the numerical procedure.

Several laser propulsion cases were calculated using the newly developed computer code. The nozzle geometry, flow configuration and optical arrangements were not optimized for rocket performance. However, some useful information was obtained from these preliminary test cases. The performance of the rocket is highly dependent on the laser focal position. The maximum velocity is larger when laser focal point moves closer to the throat. Generally speaking, the laser beam only heated a small portion of the hydrogen propellant, and the best thruster performance will not be achieved due to the two-dimensional losses. In the future, an extensive parametric study will be required to optimize the rocket performance, and one of the major goals of the study is to design the rocket to produce a more uniformly distributed temperature at the throat.

ACKNOWLEDGEMENT

The authors acknowledge Dr. C. Peters and Mr. R. Rhodes for providing valuable discussion, and Mr. J. White and Mr. M. Smith for preparing the graphs. This work has been partially supported by NASA Marshell Flight Center under Contract NAS8-36620 monitored by Mr. R. Eskridge, and Air Force Office of Scientific Research under Grant AFOSR-86-0317 monitored by Dr. R. Vondra.

REFERENCES

1. Simons, G. A., and Pirri, A. N., " The Fluid Mechanics of Pulsed Laser Propulsion," *AIAA J.*, Vol. 15, June 1977, pp. 835-842.
2. Keefer, D. R., Elkins, R., Peters, C. and Jones, L., "Laser Thermal Propulsion," in *Orbit-Raising and Maneuvering Propulsion: Research Status and Needs*, edited by L. H. Caveny, (American Institute of Aeronautics and Astronautics Inc., New York), pp. 129-148, 1984.
3. Kemp, N. H. and Root, R. G., "Analytical Study of Laser-Supported Combustion Waves in Hydrogen," *Journal of Energy*, Vol. 3, 1979, pp. 40-49.
4 Glumb, R. J. and Krier, H., "Concept and Status of Laser-Supported Rocket Propulsion," *J. Spacecraft*, Vol. 21, No.3, pp. 70-79, 1983.

5. McCay, T. D. and Dexter, C. E., "Chemical Kinetic Performance Losses for a Hydrogen Laser Thermal Thruster," AIAA paper 85-0907, June, 1985.

6. Raizer, Y. P., "Subsonic Propagation of a Light Spark and Threshold Conditions for the Maintenance of Plasma by Radiation," *Soviet Physics - JETP*, Vol. 31, 1970, pp. 1148-1154.

7 Jackson, J. P., and Nielsen, P. E., "Role of Radiative Transport in the Propagation of Laser-Supported Combustion Waves," *AIAA Journal*, Vol. 12, 1974, pp. 1498-1501.

8. Keefer, D. R., Peters, C. E. and Crowder, H. L., "A Reexamination of the Laser Supported Combustion Wave," *AIAA Journal*, Vol. 23, 1985, pp. 1208-1212.

9. Batteh, J. H. and Keefer, D. R., "Two-Dimensional Generalization of Raizer's Analysis for the Subsonic Propagation of Laser Sparks," *IEEE Transactions on Plasma Science*, vol. PS-2, 1974, pp. 122-129.

10. Keefer, D. R., Crowder, H. L. and Elkins, R., "A Two-Dimensional Model of the Hydrogen Plasma for a Laser Powered Rocket," AIAA Paper No. 82-0404, January, 1982.

11. Glumb, R. J. and Krier, H., "A Two-Dimensional Model of Laser-Sustained plasmas in Axisymmetric Flow fields," AIAA Paper No. 85-1553, July, 1985.

12. Merkle, C. L., Molvik, G. A. and Choi, Y.-H., "A Two-Dimensional Analysis of Laser Heat Addition in a Constant Absorptivity Gas," *AIAA Journal*, Vol. 23, 1985, pp. 1053-1060.

13. Merkle, C. L., Molvik, G. A. and Shaw, E. J.-H., "Numerical Solution of Strong Radiation Gasdynamic Interactions in a Hydrogen-Seedant Mixture," AIAA Paper No. 85-1554, July, 1985.

14. Jeng, S-M. and Keefer, D., "Theoretical Investigation of Laser-Sustained Argon Plasmas," Vol. 60, No. 7, pp. 2272-2279 *J. Applied Physics*, 1986.

15. Jeng, S-M. and Keefer, D., "Numerical Study of Laser-Sustained Hydrogen Plasmas in a Forced Convective Flow," AIAA paper 86-1524, May, 1986.

16. Welle, R. P., Keefer, D. R. and Peters, C. E., "Energy Conversion Efficiency in High-Flow, Laser-Sustained Argon Plasmas," AIAA paper 86-1078.

17. Keefer, D.R., Crowder H.L., and Peters, C.E., "Laser-Sustained Argon Plasmas in a Forced Convection Flows," AIAA paper No. 85-0388, January, 1985.

18. Jeng, S-M., Keefer, D., Welle, R., and Peters, C., "Numerical Study of Laser-Sustained Argon Plasmas in a Forced Convective Flow," AIAA-86-1078, May, 1986.

19. Keefer, D., Jeng, S.-M., and Welle, R., "Laser Thermal Propulsion Using Laser Sustained Plasmas," IAF-86-175, 37th Congress of the International Astronautical Federation, Innsbruck, Austria, Oct. 4-11,1986.

20. Kemp, N. H. and Root, R. G., "Analytical Study of Laser-Supported Combustion Waves in Hydrogen," NASA CR-135349, 1977.

21. Caledonia, G. E., Wu, P. K. S. and Pirri, A. N., "Radiant Energy Absorption Studies for Laser Propagation," NASA CR-134809, 1975.

22. Shyy W, "A Numerical Study of Annular Dump Diffuser Flows," *Computer Methods In Applied Mechanics And Engineering*, Vol. 53, pp. 47-65, 1985.

23. Rhie, C. M., and Chow, W. L., "Numerical Study of the Turbulent Flow Past an Airfoil with Trailing Edge Separation," *AIAA J.*, Vol. 21, No. 11, pp. 1525-1532, Nov. 1983.

24. Rhie, C. M. "A Pressure Based Navier-Stokes Slover Using the Multigrid Method, " AIAA paper 86-0207, AIAA 24th Aerospace Sciences Meeting, Reno, Nevada, Jan. 1986.

25. Patankar, S. V., *Numerical Heat Transfer and Fluid Flow*, New Hemisphere, Washington, D.C., 1980.

26. Issa, R. I., "Solution of the implicitly Discretized Fluid Flow Equations by Operator-Splitting," *J. Computational Physics*, Vol. 62, pp. 40-65, 1986.

27. Issa, R. I., Gosman, A. D., and Watkins, A.P., "The Computation of Compressible and Incompressible Recirculating Flows by a Non-iterative Implicit Scheme," *J. Computational Physics*, Vol. 62, pp. 66-88, 1986.

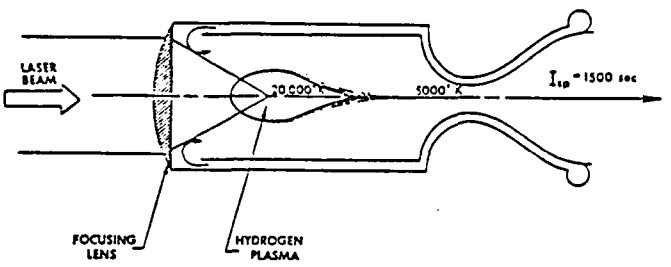

Figure 1. Schematic of a laser-sustained plasma propulsion thruster chamber.

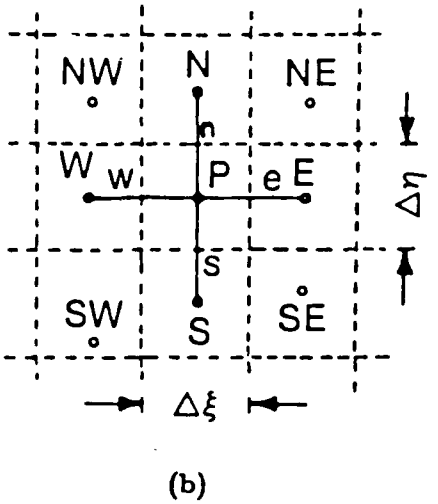

(b)

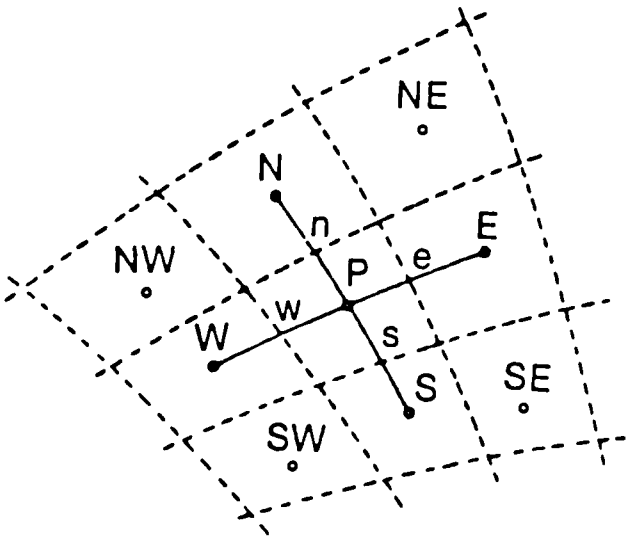

(a)

Figure 2. Finite-difference grid representation: (a) physical plane, (b) transformed plane.

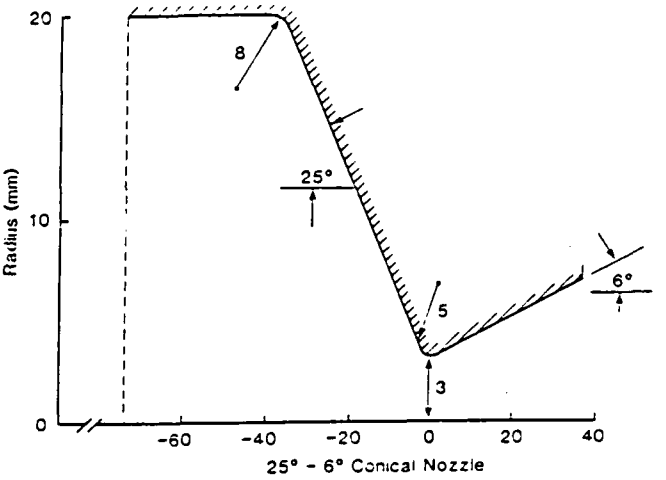

Figure 3. Conical nozzle geometry.

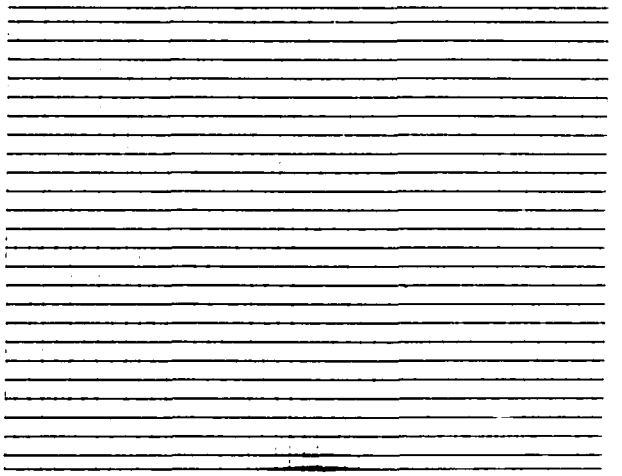

(b)

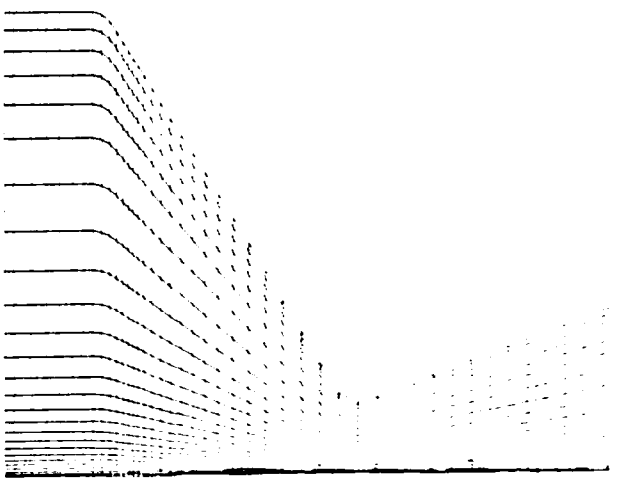

(a)

Figure 4. Schematic of grid transformation (a) physical plane, (b) transformed plane.

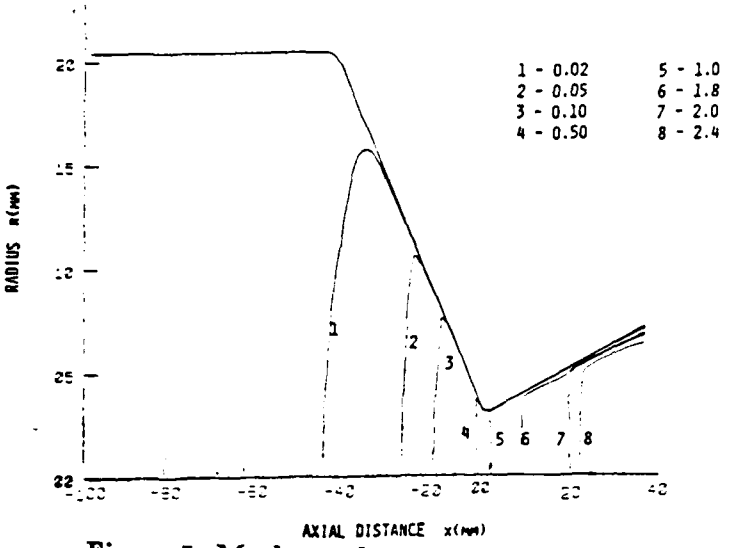

Figure 5. Mach number contours for case number 1.

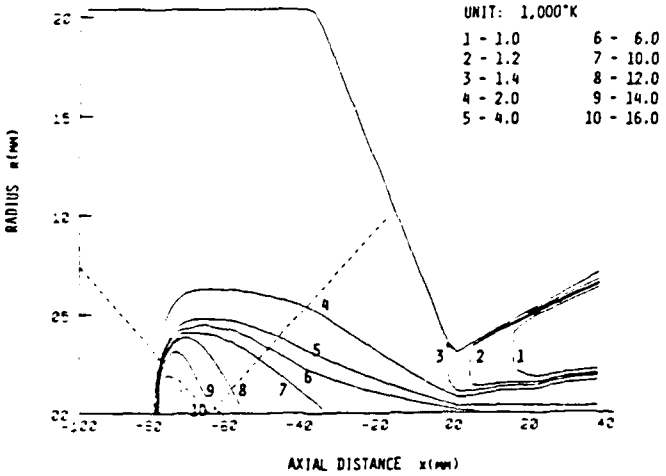

Figure 6. Temperature contours for case number 2.

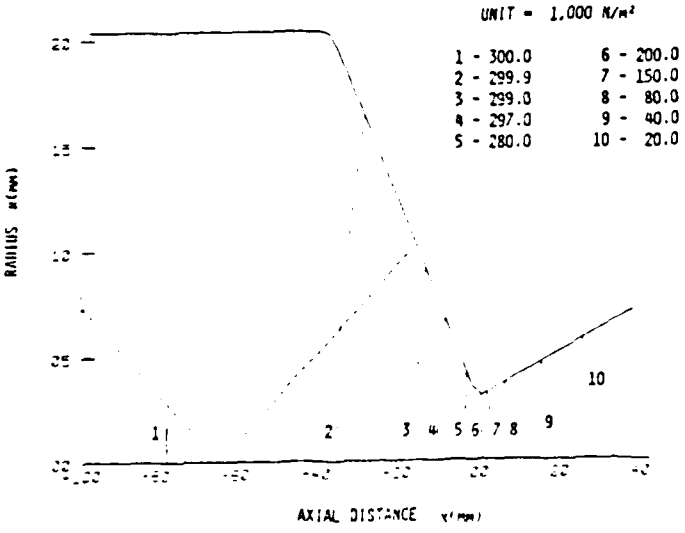

Figure 7. Pressure contours for case number 2.

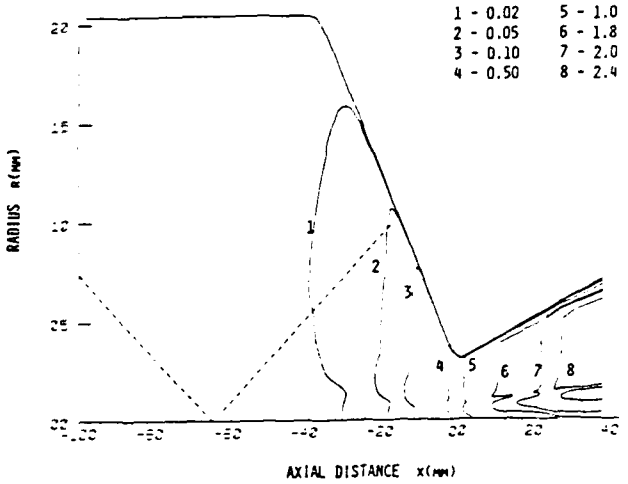

Figure 8. Mach number contours for case number 2.

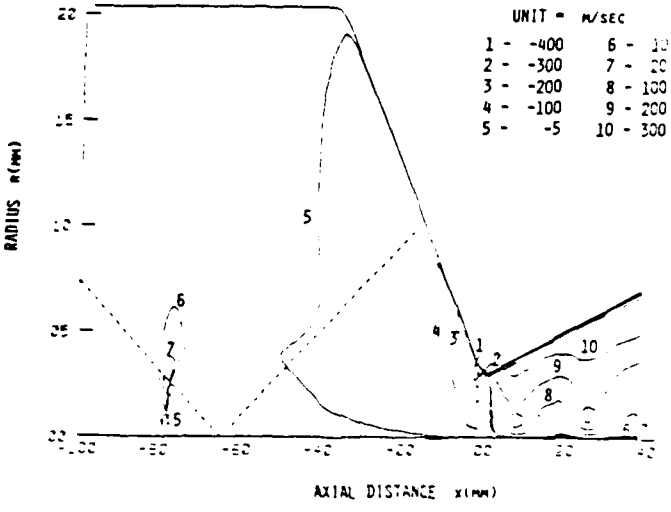

Figure 9. Radial velocity contours for case number 2.

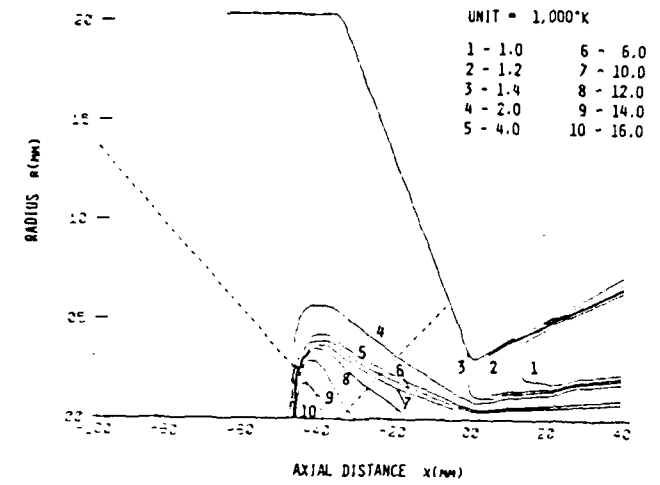

(a)

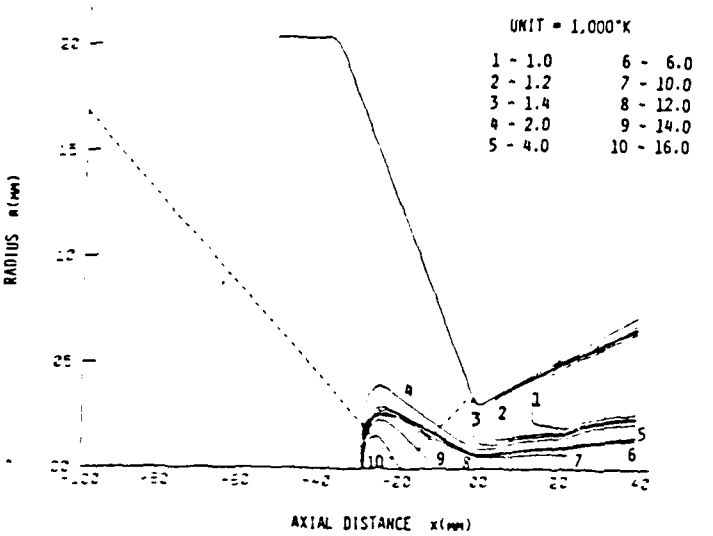

(b)

Figure 10. Temperature contours: (a) case number 4, (b) case number 5.

Table 1: Test Conditions

Case no.	Laser power (kW)	focus (mm)
1	0	
2	30	-65
3	30	-50
4	30	-35
5	30	-20

Table 2: Calculated properties for five test cases

Case no.	1	2	3	4	5
Optically thin. rad. (kW)	0.	18.6	17.9	16.0	9.9
Transmitted power (W)	0.	397	395	330	320
Max. axial vel. (m/sec)	4763	12513	13403	15643	18957
Max. temperature (K)	1500	16854	16872	16878	17293
Max. mach number	2.50	2.61	2.64	2.68	2.78
Mass flow rate (g/sec)	2.88	2.82	2.74	2.69	2.66